

# Egocentric Human Trajectory Forecasting with a Wearable Camera and Multi-Modal Fusion

Jianing Qiu<sup>1,2,3</sup>, Lipeng Chen<sup>3,†</sup>, Xiao Gu<sup>1,2</sup>, Frank P.-W. Lo<sup>2</sup>, Ya-Yen Tsai<sup>1,2,3</sup>,  
Jiankai Sun<sup>3,4</sup>, Jiaqi Liu<sup>3,5</sup> and Benny Lo<sup>2</sup>

**Abstract**—In this paper, we address the problem of forecasting the trajectory of an egocentric camera wearer (ego-person) in crowded spaces. The trajectory forecasting ability learned from the data of different camera wearers walking around in the real world can be transferred to assist visually impaired people in navigation, as well as to instill human navigation behaviours in mobile robots, enabling better human-robot interactions. To this end, a novel egocentric human trajectory forecasting dataset was constructed, containing real trajectories of people navigating in crowded spaces wearing a camera, as well as extracted rich contextual data. We extract and utilize three different modalities to forecast the trajectory of the camera wearer, i.e., his/her past trajectory, the past trajectories of nearby people, and the environment such as the scene semantics or the depth of the scene. A Transformer-based encoder-decoder neural network model, integrated with a novel cascaded cross-attention mechanism that fuses multiple modalities, has been designed to predict the future trajectory of the camera wearer. Extensive experiments have been conducted, and the results have shown that our model outperforms the state-of-the-art methods in egocentric human trajectory forecasting.

## I. INTRODUCTION

Egocentric perception has a pivotal role in agent navigation, whether it is a robot, a human, or an autonomous vehicle. With on-board cameras, forecasting the trajectory of an ego-vehicle, a mobile robot, or their surrounding agents has been actively studied in the fields of autonomous driving and robot navigation to enable better motion planning and to reduce the chances of collision [1], [2], [3]. This provides a new insight for blind navigation [4], [5], [6]. With a wearable camera as the proxy of human eyes and an algorithm (learned from sighted people walking with a wearable camera) forecasting the optimal trajectory for navigation in the next few seconds, a blind or visually impaired person can navigate through a space independently in a safer and more natural way. With a set of synchronised sensors, the forecast optimal trajectory can be communicated to the user via vibration [4] or audio [7]. On the other

<sup>1</sup>Department of Computing, Imperial College London, London SW7 2AZ, UK {jianing.qiu17, xiao.gu17, y.tsai17}@imperial.ac.uk

<sup>2</sup>The Hamlyn Centre, Imperial College London, London SW7 2AZ, UK {po.lo15, benny.lo}@imperial.ac.uk

<sup>3</sup>Tencent Robotics X, Shenzhen 518057, China lipengchen@tencent.com

<sup>4</sup>Department of Aeronautics and Astronautics, Stanford University, CA 94305, USA jksun@stanford.edu

<sup>5</sup>Institute of Medical Robotics, Shanghai Jiao Tong University, Shanghai 200240, China 1jq64408@sjtu.edu.cn

†corresponding author

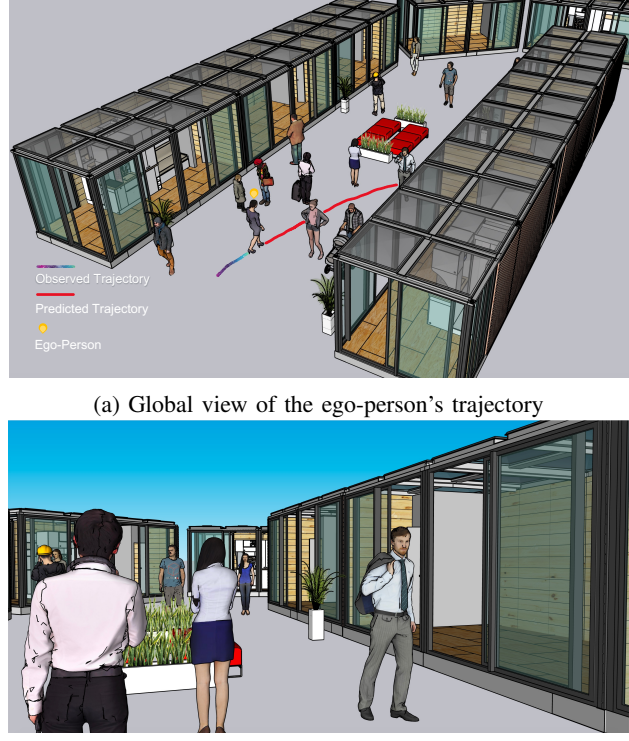


Fig. 1: Illustration of the egocentric human trajectory forecasting. An ego-person (a person with a wearable camera) is walking around in a crowded space (e.g., in a shopping mall). The wearable camera, which has an egocentric view, continuously captures close-up details of the wearer's surroundings. In this work, we aim to predict the ego-person's trajectory by only using the contextual cues captured by the wearable camera and the ego-person's past trajectory.

hand, humans tend to unconsciously follow certain social rules, such as maintaining a comfortable distance with others, and keeping following the people in front of them if not in a rush while walking in crowded spaces. These socially polite ways of navigation are common in human navigation. For a mobile robot, if it can imitate such human navigation behaviours, the robot could better blend itself into human-centric environments while moving in shared spaces with humans. The human navigation behaviours distilled from the egocentric perception data of humans navigating in the real world therefore has the potential to be transferred to mobile robots, enabling socially compliant robot navigation [8].

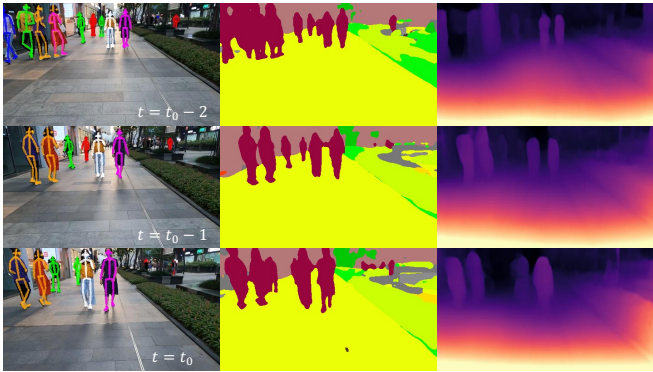


Fig. 2: Visual cues for forecasting the trajectory of the camera wearer. (Left) the past trajectories of nearby people (formed by using their poses at each time point. We have also investigated the use of their center body points or bounding boxes to form their trajectories in the 2D pixel space). (Middle) the segmented semantics of the scene at each time point in the observation period. (Right) the estimated depth of the scene at each time point in the observation period.

However, such data is currently lacking and limited research has been carried out in forecasting the trajectory of the camera wearer [9], [10], [11], [12]. Most human trajectory forecasting methods are targeted for scenarios captured from a bird-eye view or by a static camera [13], [14], [15], [16], [17], [18], [19], [20], [21], [22]. Different from these views, egocentric view brings up the opportunity of understanding how humans perceive the surroundings, and initiate/execute the responsive actions. Such embodied knowledge fully considers the relationship between the agent itself and the close-up contextual information, such as the poses of nearby people and their trajectories, and the sizes of obstacles. These close-up details are crucial for forecasting a safe trajectory. Nevertheless, to the best of our knowledge, there is currently no effort that has been made to forecast the camera wearer’s trajectory with these close-up contextual cues. From the perspective of applicability, it is also more practical to implement visual navigation assistance using an egocentric view than using a bird-eye or static camera view.

In light of these, in this work, we propose and address the task of forecasting the trajectory of an egocentric camera wearer in crowded spaces. Fig. 1 provides an illustration of this task. Specifically, given a period of observation, the task is to forecast the camera wearer’s trajectory (expressed in the 3D world coordinates with both position and orientation) using cues available in the observation period. We adopt the past trajectory of the camera wearer as the basic input, and meanwhile, utilize the contextual information (as shown in Fig. 2), such as the trajectories of nearby people, and the scene semantics or the depth of the scene, to forecast the trajectory of the camera wearer. To this end, an encoder-decoder structure is proposed, in which multiple encoder streams are used to encode different input modalities, and a novel cascaded cross-attention mechanism is then used to fuse the resulting encodings. The decoder receives the

fused encodings, and then decodes the future trajectory in an autoregressive manner. The effectiveness of using different modalities has been thoroughly studied in this work.

In a nutshell, the contributions of this work include:

- A novel in-the-wild egocentric human trajectory forecasting dataset has been constructed.
- Three different types of modalities are proposed and their effectiveness has been evaluated for egocentric human trajectory forecasting.
- A Transformer-based encoder-decoder framework integrated with a novel cascaded cross-attention mechanism has been designed to forecast the trajectory of the camera wearer in the egocentric setting.

## II. RELATED WORK

In this section, we review prior work in human trajectory prediction, including in both non-egocentric and egocentric scenarios.

### A. Non-Egocentric Human Trajectory Prediction

Most human trajectory prediction studies are focused on scenes captured from a bird-eye view or by a static camera, i.e., non-egocentric scenarios, with targeted applications, such as intelligent surveillance systems and crowd behavior monitoring. The majority of the work considers modelling pedestrian walking dynamics to approach this task. Early work resorted to hand-craft features such as social force [23]. Recent studies have shifted to neural network-based approaches. Social-LSTM [13] proposed to use social pooling layers to model human-human interactions to better predict each person’s trajectory. Social-GAN [14] later employed adversarial learning and a variety loss to encourage the diversity of the predicted trajectories. Both SoPhie [15] and Social-BiGAT [16] leveraged social interactions between pedestrians and scene context to generate a distribution of a pedestrian’s future trajectories. Predicting multiple future trajectories has also been attempted in [18] with the use of multi-scale location decoders. Liang et al. [17] proposed to predict a pedestrian’s future trajectory and activities jointly. Such a joint modeling was shown to be effective to enhance trajectory prediction performance. Mangalam et al. [19] proposed to predict pedestrian trajectories conditioned on their destinations. A conditional 3D attention mechanism was proposed in [20] to improve pedestrian trajectory prediction.

Transformer [24] recently has established new state-of-the-arts in a series of vision and language tasks. Few studies have also exploited the transformer-based architecture for pedestrian trajectory prediction. STAR [21] predicts pedestrian trajectories with only the attention mechanism, which is achieved by a graph-based spatial transformer and a temporal transformer. AgentFormer [22], a transformer-based framework, jointly models temporal and social dimensions in human motion dynamics to predict future trajectories. Our model is also based on transformer, but we differ from them in that 1) we target for egocentric scenarios, and 2) our model encodes multiple modalities with a novel cascaded cross-attention mechanism, whereas their models are designed

to use the past trajectories as the only cue for the future trajectory prediction.

### B. Egocentric Human Trajectory Prediction

In egocentric scenarios, based on the types of used visual sensors, human trajectory prediction can be categorized into the vehicle-mounted camera scenario and the wearable camera scenario.

1) *Vehicle-Mounted Camera Scenario*.: In the field of autonomous driving, pedestrian trajectory prediction has been actively researched in order to ensure that an autonomous vehicle can react promptly to avoid collision when encountering pedestrians on road [25], [26], [27], [28], [29], [30]. Some research has also studied the prediction of a pedestrian's intent of crossing or not crossing the road [31], [32], and the detection of traffic accident by predicting pedestrians' future locations [33]. As the vehicles are mainly on the road, in the images/videos captured by a vehicle-mounted camera, the pedestrians often appear on the sidewalks, and therefore are mainly in the left or right section of the images/videos, or in the middle when the vehicle is at an intersection. These scenes hence differ from those captured by a wearable camera, as the places the camera wearer can visit and enter are different from vehicles and the locations of nearby people can be in close proximity to the camera wearer. For example, the camera wearer can walk in a long distance following the person in front, which can rarely be found in vehicle-mounted camera scenarios. The motion dynamics of a camera wearer and an ego-vehicle also differs, resulting in the changes of the scene captured by their respective camera being also different.

2) *Wearable Camera Scenario*.: Among work using wearable cameras, Yagi et al. [34] first proposed the task of future person localization in egocentric videos. In their work, a multi-stream 1D convolution-deconvolution (1D Conv-DeConv) network was designed to utilize a pedestrian's past poses, locations and scales, as well as ego-motion to infer his/her future locations. In [35], a GRU-CNN-based framework was proposed to conduct future person localization. An LSTM-based encoder-decoder framework was utilized in [36] to predict human trajectory in indoor environments. The above work, similar to those in the vehicle-mounted camera scenario, is focused on predicting the trajectories of the pedestrians captured by egocentric cameras, which is different from our work. Our work is to predict the trajectory of the camera wearer rather than those of pedestrians, which could benefit the blind navigation as well as the socially compliant robot navigation.

Nevertheless, little research has been carried out in predicting the camera wearer's trajectory. An early attempt was made by Park et al. [9], who used stereo images and an EgoRetinal map to predict the camera wearer's future path. Given a single egocentric image, a nearest-neighbor based search approach was used in [10] to predict the future trajectory. The search was based on the measured deep-feature similarity between images. Camera wearer trajectory prediction has also been studied in the context of playing

basketball. Bertasius et al. [11] proposed to use a future CNN and a goal verifier network followed by an inverse synthesis procedure to estimate a basketball player's motion. In [12], egocentric videos were used and basketball players' trajectories were predicted by a retrieval-based method. Although our work also predicts the trajectory of the camera wearer, we differ from them in that 1) we model the interactions between the camera wearer and the people in his/her close vicinity in both crowded indoor and outdoor spaces; 2) rich visual features, such as scene semantics and depth information, are leveraged to aid trajectory prediction; 3) and without bells and whistles, our method, based on a simple encoder-decoder structure and a novel cascaded cross-attention mechanism, has shown to be effective in fusing multiple contextual cues and accurately predicting the trajectory of the camera wearer.

## III. METHOD

### A. Problem Formulation

We formulate the task of predicting the trajectory of an egocentric camera wearer as to learn a function  $\phi_\theta : (\mathcal{Y}, \mathcal{Z}) \rightarrow \hat{\mathcal{Y}}$ , which takes the past trajectory  $\mathcal{Y}$  of the camera wearer and some contextual cues  $\mathcal{Z}$  as inputs, and outputs the camera wearer's future trajectory  $\hat{\mathcal{Y}}$ .

### B. Ego-Trajectory Forecasting with Multiple Modalities

People navigate in crowded spaces with social etiquette, and the movement of each individual is influenced by those of nearby people. Therefore, in predicting the trajectory of a camera wearer, the trajectories of people in his/her close vicinity can play an important role. Hence, we use the nearby people's trajectories  $\mathcal{J}$  as one of the cues for forecasting the camera wearer's trajectory. In addition, understanding the scene semantics (e.g., walkable areas such as the floor, and obstacles such as walls) can also aid trajectory forecasting. We therefore use scene semantic segmentation  $\mathcal{S}$  as another cue for camera wearer trajectory forecasting. Hence, we have  $\mathcal{Z} = [\mathcal{J}, \mathcal{S}]$ .

We have also experimented on the depth information, and used depth estimation  $\mathcal{D}$  as an alternative to the scene semantic segmentation, i.e.,  $\mathcal{Z} = [\mathcal{J}, \mathcal{D}]$ . As the methodologies of processing and fusing scene segmentation and depth estimation with other two modalities are similar, in this section, we mainly focus on the use of the past trajectory  $\mathcal{Y}$  of the camera wearer, those of nearby people  $\mathcal{J}$ , and the scene semantic segmentation  $\mathcal{S}$ . Experimental results of using the depth estimation will be present in Section IV-E.2.

Concretely, given a period of observation (past)  $T_{\text{obs}}$ , the camera wearer's past trajectory  $\mathcal{Y} \in \mathbb{R}^{T_{\text{obs}} \times 7}$  is formed chronologically using the camera position ( $\mathbf{p} \in \mathbb{R}^{T_{\text{obs}} \times 3}$ ) and orientation ( $\mathbf{o} \in \mathbb{R}^{T_{\text{obs}} \times 4}$ , as quaternion) at each time point  $t \in (t_0 - T_{\text{obs}} + 1, \dots, t_0)$  where  $t_0$  is the end of the observation period. The past trajectories of nearby people  $\mathcal{J} = \sum_{n=1}^N J_n$  where  $N$  is the number of nearby people and  $J_n \in \mathbb{R}^{T_{\text{obs}} \times d}$  is each nearby person's trajectory projected in the 2D pixel space (the viewpoint of the camera wearer) during the time period  $t \in (t_0 - T_{\text{obs}} + 1, \dots, t_0)$ , and  $d$  is the dimension of the cue we use to represent the nearby people's trajectories. We

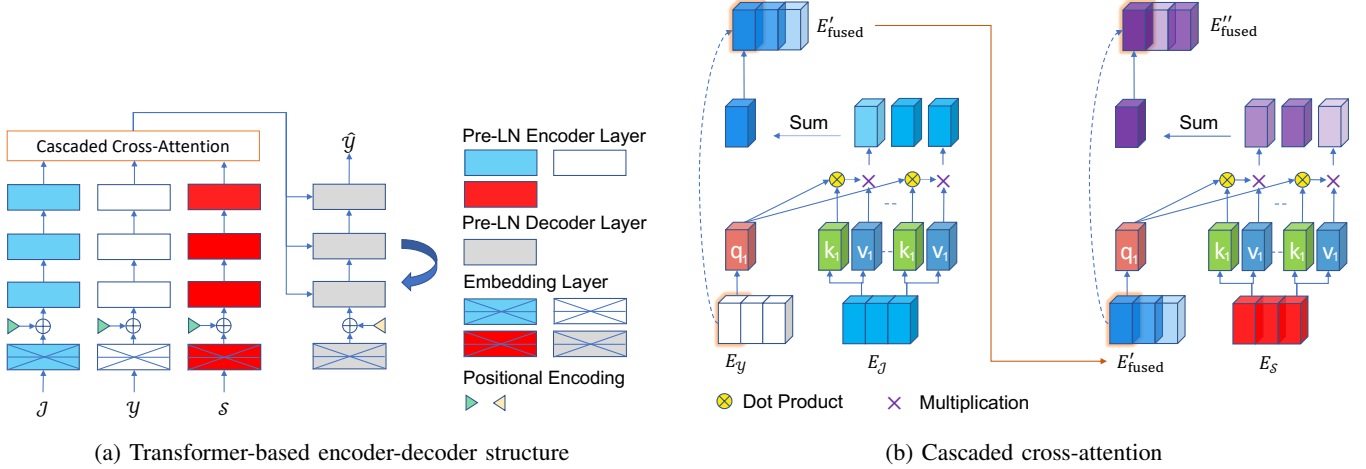


Fig. 3: (a) Overview of the model structure. The model is composed of three encoder streams, each with three Pre-LN Transformer layers to encode an input modality, and a single decoder stream to decode the future trajectory of the camera wearer in an autoregressive manner. A cascaded cross-attention mechanism is designed to fuse the encodings of multiple modalities. (b) Illustration of the cascaded cross-attention mechanism.

#### Algorithm 1: Cascaded Cross-Attention Mechanism

```

Data:  $E_{\mathcal{Y}}$ ,  $E_{\mathcal{J}}$ , and  $E_{\mathcal{S}}$ 
Result:  $E'_{\text{fused}}$ : the fused encodings of all input modalities.

/* LN is Layer Normalization.  $W_q$ ,  $W_k$ , and  $W_v$  are learnable matrices.  $1/\sqrt{d_k}$  is the scaling factor. */
1  $E_{\text{fused}} \leftarrow E_{\mathcal{Y}}$ ;
2  $E_{\text{others}} \leftarrow [E_{\mathcal{J}}, E_{\mathcal{S}}]$ ;
3 for  $E$  in  $E_{\text{others}}$  do
4    $E_{\text{fused}}' \leftarrow \text{LN}(E_{\text{fused}})$ ;
5    $E_{\text{fused}} \leftarrow \text{softmax}(W_q E_{\text{fused}}' (W_k E)^T / \sqrt{d_k}) W_v E + E_{\text{fused}}$ ;
6 end

```

mainly use a nearby person's pose to form his/her trajectory, but the use of his/her center body point, as well as his/her bounding box has also been investigated. For scene semantic segmentation, we encode the corresponding segmentation mask at each time point in the observation period into a  $k$ -dimensional vector, i.e.,  $\mathcal{S} \in \mathbb{R}^{T_{\text{obs}} \times k}$ . Similarly, if the depth images are used, we have  $\mathcal{D} \in \mathbb{R}^{T_{\text{obs}} \times k}$ .

Finally, given a prediction period  $T_{\text{pred}}$ , the future trajectory of the camera wearer  $\hat{\mathcal{Y}} \in \mathbb{R}^{T_{\text{pred}} \times 7}$  can be predicted using  $\phi_{\theta}(\mathcal{Y}, \mathcal{Z})$  where  $\mathcal{Z} = [\mathcal{J}, \mathcal{S}]$  or  $\mathcal{Z} = [\mathcal{J}, \mathcal{D}]$ .

#### C. Model Structure

We implement  $\phi_{\theta}$  as a Transformer based encoder-decoder neural network model containing a novel cascaded cross-attention mechanism to fuse encodings of different modalities. Fig. 3 shows the model structure. Each modality is encoded by a separate encoder stream, and each stream con-

tains three Pre-LN Transformer layers [37]. After encoding, the inputs  $\mathcal{Y}$ ,  $\mathcal{J}$  and  $\mathcal{S}$  are transformed into  $E_{\mathcal{Y}}$ ,  $E_{\mathcal{J}}$ , and  $E_{\mathcal{S}}$ , respectively. We then utilize a cascaded cross-attention mechanism (see Algorithm 1) to fuse them. The fused encoding  $E'_{\text{fused}}$  is then fed into the decoder. In inference, we use greedy decoding to decode the future trajectory, and based on the experiments, using greedy decoding in training is able to increase the trajectory prediction accuracy during inference. This increase is also observed in [22]. Therefore, in both training and inference, the decoder decodes the future trajectory of the camera wearer in a greedy autoregressive manner. We name our model as CXA-Transformer (Cascaded Cross-Attention Transformer).

## IV. EXPERIMENT

### A. Dataset

A novel egocentric human trajectory forecasting dataset has been constructed. To the best of our knowledge, this new dataset is the first of its kind in the community.

1) *Data Collection*: A camera wearer was wearing a Go-Pro Hero 9 Black camera while walking around in crowded spaces, such as a large shopping mall. Six unique areas were chosen to collect the data. Both indoor and outdoor scenarios were covered. For outdoor scenarios, data was collected in busy city areas where vehicles are not allowed to enter. The camera was mounted on the chest of the wearer and facing forward. The camera recorded egocentric videos with a resolution of  $1920 \times 1080$  at 30 fps.

2) *Data Pre-Processing*: We run ORB-SLAM3 [38] to obtain the trajectories of the camera wearer from the recorded egocentric monocular RGB videos. We then used ffmpeg to extract frames from the videos and set the resolution of each frame to  $480 \times 270$ . AlphaPose [39] was then used to detect and track nearby people appearing in each frame. For each tracked nearby person, we used his/her detected pose in each frame to form his/her trajectory in the 2D

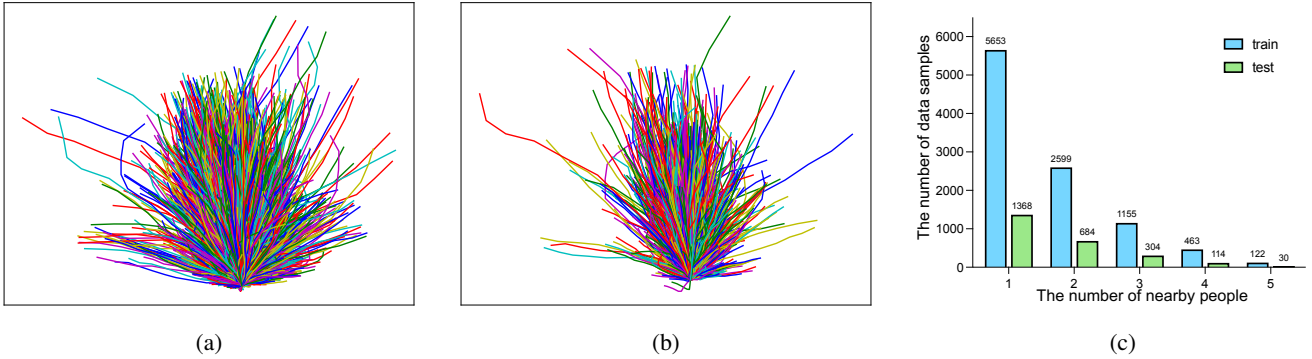


Fig. 4: (a) The distribution of the training trajectories projected onto the x and y coordinate plane (9,992 trajectories in total). (b) The distribution of the test trajectories projected onto the x and y coordinate plane (2,500 trajectories in total). (c) The number of data samples with respect to the different number of nearby people.

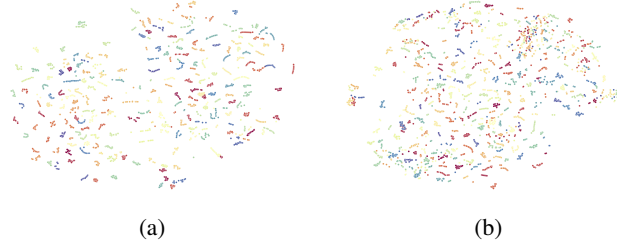


Fig. 5: t-SNE visualization of the encodings of scene semantic segmentation masks (a) and depth images (b). Each cluster is the encodings of the segmentation masks or the depth images of one trajectory in the observation period (best viewed in zoom in). Each encoding is represented by a dot. Same color means they are from the same trajectory. For visualization purpose, 1) we use 15 frames for each trajectory, i.e., 10fps, and the used frames of 2fps are within these 15 frames; 2) 200 samples are randomly chosen from the test set, as shown in (a) and (b). It can be observed that the encodings learned from the designed autoencoder are discriminative between different trajectories, and the encodings of scene semantic segmentation are more discriminative than those of depth images, which is also confirmed by the experiments discussed in Section IV-E.2

pixel space. We also used the center of his/her neck and hip keypoints to represent his/her center body point in each frame. The center body point and the detected bounding box of a nearby person are used as alternatives to the pose to form his/her trajectory. PSPNet [40] was used to segment scene semantics. The parsed scene semantics of each frame is represented by a segmentation mask with the same size as the RGB frame. After segmentation masks were obtained, we trained an autoencoder to encode each mask into a  $k$ -dimensional vector. Monodepth2 [41] was used to estimate the depth from the monocular RGB frames. Similar to the segmentation mask, we trained a separate autoencoder to encode each depth image into a  $k$ -dimensional vector.

The timestamps of the camera wearer’s trajectory are aligned with those of video frames, and we reduce the frame

rate to 2fps. Each trajectory of the camera wearer is 5 seconds long (i.e., 10 time points), each of which records a sequence of camera poses and these poses are expressed in relative to the initial pose of that sequence.

In total, the dataset contains 12,492 unique trajectories, and we use 9,992 for training and the rest 2,500 for testing. The distribution of the trajectories in the training and test sets are shown in Fig. 4a and Fig. 4b, respectively. We limit the maximum number of nearby people to 5 in the dataset. Fig. 4c shows the number of data samples with respect to the different number of nearby people. We use t-SNE [42] to visualize the encoded vectors (by the respective autoencoder) of segmentation masks and depth images in Fig 5. We name our dataset as TISS (the initial of the four institutions involved in this work).

### B. Implementation Details

Our model was implemented using PyTorch. We used 4 attention heads in the Pre-LN Transformer layers and the cascaded cross-attention module. Hidden layer dimension of the Pre-LN Transformer’s feed forward sub-layers was set to 2,048. The embedding layers transform modalities of different dimensions to the same dimension of 512. The implementation of PSPNet and its pre-trained model were adopted from [43]. We set the observation time  $T_{\text{obs}}$  to 3 time points (at 2fps, it is equal to 1.5 s) and the prediction time  $T_{\text{pred}}$  to 7 time points (at 2fps, it is equal to 3.5 s). We used 26 body keypoints to represent a nearby person’s pose. We used zero padding to pad those data samples which have the number of nearby people less than 5. Therefore,  $d$  was set to 260 when body pose was used, and  $d$  was 10 and 20 respectively, if the center body point and the bounding box were used.  $k$  was set to 648. We trained our model for 300 epochs using Adam optimization [44]. The batch size was set to 1,024 with a learning rate of 5e-5.

### C. Baselines

We compared the performance of egocentric human trajectory prediction of our **CXA-Transformer** model with the following baseline methods:

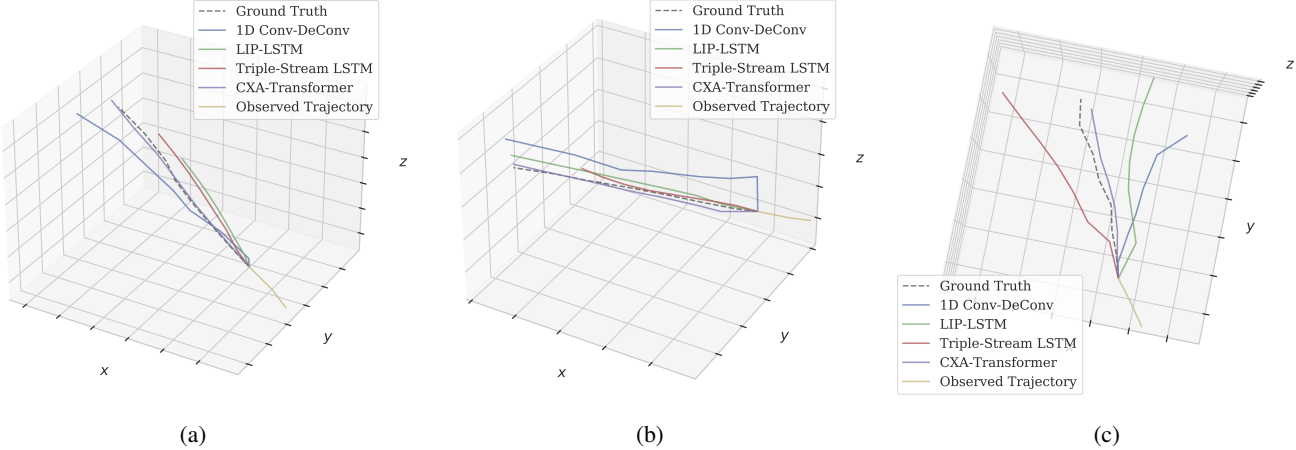


Fig. 6: Visualization of the predicted trajectories of different methods, the ground truth, and the observed trajectory. The predicted trajectory of our CXA-Transformer better aligns with the ground truth compared to those of baselines.

- **1D Conv-DeConv** [34]: A multi-stream 1D convolution-deconvolution framework originally proposed for future pedestrian localization in egocentric videos. We adapt it to be compatible with different modalities and their different dimensions in our dataset.
- **Triple-Stream LSTM**: An LSTM-based encoder-decoder framework with three encoder streams and one decoder stream. Different input modalities are merged using two fully connected layers (one for hidden states, and the other for cell) before being fed into the decoder.
- **LIP-LSTM** [36]: A single stream LSTM-based encoder-decoder framework originally proposed for predicting the location and movement trajectory of pedestrians captured in egocentric videos. We concatenate input modalities and then feed the resulting vector to its encoder. Future trajectory is then predicted by its decoder.

#### D. Evaluation Metrics

We used MSE to measure the future trajectory prediction error of each method (i.e., 7 time points in the case of predicting 3.5s into the future). Apart from the overall prediction error, we also separately report the error of position and orientation prediction. In addition, we also compared the performance of each method on different prediction horizons, i.e., 1.0s, 1.5s, 2.0s, 2.5s, and 3.0s.

#### E. Results

1) *Comparison with the State-of-the-Art*: Table I summarizes the results of our method and the baselines on the task of egocentric human trajectory forecasting. Our CXA-Transformer achieves the lowest prediction error in terms of the estimated future position and orientation of the camera wearer. Its overall prediction error is nearly as half of the second best method’s prediction error. Fig. 6 shows three examples of the predicted trajectories of different methods as well as the ground truth and the observed trajectory. It can be seen that the predicted trajectory of our model aligns better

TABLE I: Comparison with the State-of-the-Art Methods

Method	Position	Orientation	Overall
1D Conv-DeConv [34]	7.09e-2	1.77e-3	3.14e-2
Triple-Stream LSTM	6.40e-2	7.37e-4	2.78e-2
LIP-LSTM [36]	6.67e-2	4.54e-4	2.89e-2
CXA-Transformer (Ours)	<b>3.54e-2</b>	<b>4.27e-4</b>	<b>1.54e-2</b>

TABLE II: Results of Different Prediction Horizons

Method	Pred@1.0s	Pred@1.5s	Pred@2.0s	Pred@2.5s	Pred@3.0s
1D Conv-DeConv [34]	3.29e-3	5.92e-3	9.85e-3	1.55e-2	2.25e-2
Triple-Stream LSTM	3.70e-3	6.74e-3	1.08e-2	1.59e-2	2.15e-2
LIP-LSTM [36]	6.11e-3	9.01e-3	1.26e-2	1.72e-2	2.25e-2
CXA-Transformer (Ours)	<b>3.15e-3</b>	<b>5.00e-3</b>	<b>7.31e-3</b>	<b>1.02e-2</b>	<b>1.36e-2</b>

with the ground truth than those of baselines. In Fig. 6a, the predicted trajectory of the CXA-Transformer almost perfectly matches with the ground truth. In Fig. 6b, although the prediction of the Triple-Stream LSTM aligns well with the ground truth at the beginning, it actually underestimates the walking speed of the camera wearer, and its predicted trajectory also deviates in the end, whereas the predicted trajectory of our CXA-Transformer is close to the ground truth and ends almost at the same location as the ground truth. In the example shown in Fig. 6c, the ground truth trajectory is winding, which makes the prediction hard. The predicted trajectories of all three baselines deviate largely from the ground truth, and only the CXA-Transformer is able to predict a close trajectory in this case.

Table II shows the results of predicting future trajectory at various horizons. The proposed CXA-Transformer also shows better performance than all baselines at shorter prediction horizons. It is worth noting that at very short prediction horizons, e.g., 1.0s, and 1.5s, the prediction error of the CXA-Transformer is not significantly lower than those of the baselines. However, when the prediction horizon extends, the margin of prediction error between the CXA-Transformer

TABLE III: Ablation Studies of Using Different Types of Modalities as the Input to CXA-Transformer

Modality	Position	Orientation	Overall
$\mathcal{Y}$	1.06e-1	7.10e-4	4.60e-2
$\mathcal{Y} + \mathcal{C}$	1.01e-1	6.56e-4	4.36e-2
$\mathcal{Y} + \mathcal{B}$	9.28e-2	6.78e-4	4.01e-2
$\mathcal{Y} + \mathcal{P}$	9.06e-2	6.31e-4	3.92e-2
$\mathcal{Y} + \mathcal{S}$	6.23e-2	6.00e-4	2.70e-2
$\mathcal{Y} + \mathcal{D}$	7.02e-2	6.66e-4	3.05e-2
$\mathcal{Y} + \mathcal{C} + \mathcal{S}$	3.73e-2	4.57e-4	1.63e-2
$\mathcal{Y} + \mathcal{B} + \mathcal{S}$	3.61e-2	4.38e-4	1.57e-2
$\mathcal{Y} + \mathcal{P} + \mathcal{S}$	<b>3.54e-2</b>	<b>4.27e-4</b>	<b>1.54e-2</b>
$\mathcal{Y} + \mathcal{C} + \mathcal{D}$	4.93e-2	5.26e-4	2.14e-2
$\mathcal{Y} + \mathcal{B} + \mathcal{D}$	4.76e-2	5.36e-4	2.07e-2
$\mathcal{Y} + \mathcal{P} + \mathcal{D}$	4.81e-2	5.37e-4	2.09e-2

and baselines starts to increase evidently, showing that our CXA-Transformer is better at predicting at long horizons.

2) *Ablation Studies*: We further studied the effectiveness of each input modalities in predicting egocentric human trajectory. Table III summarizes the results of using different number of modalities as the input to the CXA-Transformer. Compared to using the camera wearer’s past trajectory  $\mathcal{Y}$  as the only cue for prediction, adding the trajectories of nearby people (whether using their center body point  $\mathcal{C}$ , bounding box  $\mathcal{B}$ , or pose  $\mathcal{P}$ ), or the scene semantics  $\mathcal{S}$ , or the depth information  $\mathcal{D}$  can reduce the prediction error. When adding the cues of both nearby people and the environment, the prediction error can be further reduced. The CXA-Transformer achieved the lowest prediction error with the  $\mathcal{Y}$ ,  $\mathcal{P}$ , and  $\mathcal{S}$  as its input. The prediction error of using the depth information is higher than that of using the scene semantics as the depth is less discriminative than the scene segmentation as shown in Fig. 5. We show in Fig. 7 the accuracy of the CXA-Transformer with different structure settings, i.e., varying the number of Pre-LN layers, the dimension of the output of the embedding layers and that of the feed-forward sub-layers, and also the number of attention heads.

## V. DISCUSSION

With a person navigating in crowded spaces wearing a camera for data collection, the nearby people’s navigation behaviors are less likely to be affected. Therefore, our dataset can be used to understand and model human navigation behaviours more precisely in egocentric settings compared to the data collected by a mobile robot. Our proposed end-to-end approach that utilizes multiple input modalities has also shown to be effective in forecasting the trajectory of the camera wearer. However, in order to realize the ultimate objective of assisting blind navigation and achieving socially compliant robot navigation by transferring the trajectory forecasting ability learned from the sighted people data, two problems need to be addressed: 1) domain adaption and 2)

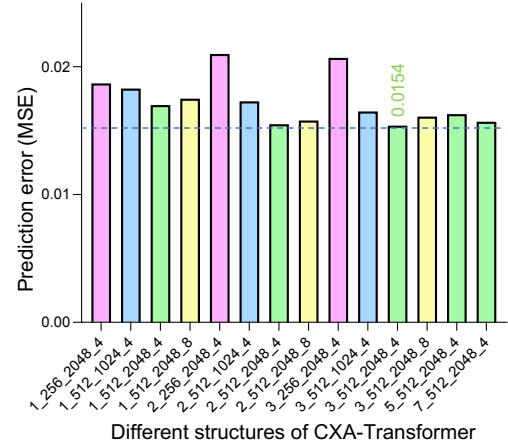


Fig. 7: Accuracy of the CXA-Transformer with the different number of Pre-LN layers (NP), different embedding dimensions (DE), different dimensions of the feed-forward sub-layer (DF), and different number of attention heads (NA). Accuracy is reported with the use of  $\mathcal{Y} + \mathcal{P} + \mathcal{S}$  as the input. X label is represented in the format of NP\_DE\_DF\_NA.

domain generalization. Specifically, a model learned from the sighted people data has to be adaptive to a different user, as different people have different height, gait, walking speed, and reaction speed. This domain shift further enlarges when transferring to a mobile robot. Developing an effective adaptive method is therefore needed. In addition, although it is possible to collect a large volume of data of sighted camera wearers walking around in different places, it is very unlikely that all scenarios a person/robot will encounter are captured. Therefore, it is worth developing a model that is able to generalize to different scenes to reduce prediction errors when facing a scene that has never been seen before. It is also worth noting that in a sighted people wearing a camera scenario, forecasting his/her trajectory may also be useful to provide more interactive and immersive AR/VR experience, and hence future research can also be carried out in this direction.

## VI. CONCLUSION

In this work, we address the problem of forecasting the trajectory of camera wearers in the egocentric setting. To this end, a novel in-the-wild egocentric human trajectory forecasting dataset has been constructed, containing trajectories of the camera wearer in the 3D space and trajectories of nearby people in the 2D pixel space, as well as the segmented scene semantics and the estimated depth of the environment captured by the wearable camera. A transformer-based encoder-decoder model has been designed with a novel cascaded cross-attention mechanism to fuse features of different modalities. The results have shown that our model is able to reliably forecast the trajectory of camera wearers at long prediction horizons.

## REFERENCES

[1] M. Everett, Y. F. Chen, and J. P. How, “Motion planning among dynamic, decision-making agents with deep reinforcement learning,” in *2018 IEEE/RSJ International Conference on Intelligent Robots and Systems (IROS)*. IEEE, 2018, pp. 3052–3059.

[2] C. Chen, Y. Liu, S. Kreiss, and A. Alahi, “Crowd-robot interaction: Crowd-aware robot navigation with attention-based deep reinforcement learning,” in *2019 International Conference on Robotics and Automation (ICRA)*. IEEE, 2019, pp. 6015–6022.

[3] F. Marchetti, F. Becattini, L. Seidenari, and A. Del Bimbo, “Multiple trajectory prediction of moving agents with memory augmented networks,” *IEEE Transactions on Pattern Analysis and Machine Intelligence*, 2020.

[4] H.-C. Wang, R. K. Katschmann, S. Teng, B. Araki, L. Giarré, and D. Rus, “Enabling independent navigation for visually impaired people through a wearable vision-based feedback system,” in *2017 IEEE international conference on robotics and automation (ICRA)*. IEEE, 2017, pp. 6533–6540.

[5] E. OhnBar, K. Kitani, and C. Asakawa, “Personalized dynamics models for adaptive assistive navigation systems,” in *Conference on Robot Learning*. PMLR, 2018, pp. 16–39.

[6] Y. Zhao, E. Kupferstein, B. V. Castro, S. Feiner, and S. Azenkot, “Designing air visualizations to facilitate stair navigation for people with low vision,” in *Proceedings of the 32nd annual ACM symposium on user interface software and technology*, 2019, pp. 387–402.

[7] google, “Project guideline: Enabling those with low vision to run independently,” 2021.

[8] H. Kretzschmar, M. Spies, C. Sprunk, and W. Burgard, “Socially compliant mobile robot navigation via inverse reinforcement learning,” *The International Journal of Robotics Research*, vol. 35, no. 11, pp. 1289–1307, 2016.

[9] H. S. Park, J.-J. Hwang, Y. Niu, and J. Shi, “Egocentric future localization,” in *Proceedings of the IEEE Conference on Computer Vision and Pattern Recognition*, 2016, pp. 4697–4705.

[10] K. K. Singh, K. Fatahalian, and A. A. Efros, “Krishnacam: Using a longitudinal, single-person, egocentric dataset for scene understanding tasks,” in *2016 IEEE Winter Conference on Applications of Computer Vision (WACV)*. IEEE, 2016, pp. 1–9.

[11] G. Bertasius, A. Chan, and J. Shi, “Egocentric basketball motion planning from a single first-person image,” in *Proceedings of the IEEE Conference on Computer Vision and Pattern Recognition*, 2018, pp. 5889–5898.

[12] S. Su, J. Pyo Hong, J. Shi, and H. Soo Park, “Predicting behaviors of basketball players from first person videos,” in *Proceedings of the IEEE Conference on Computer Vision and Pattern Recognition*, 2017, pp. 1501–1510.

[13] A. Alahi, K. Goel, V. Ramanathan, A. Robicquet, L. Fei-Fei, and S. Savarese, “Social lstm: Human trajectory prediction in crowded spaces,” in *CVPR*, 2016, pp. 961–971.

[14] A. Gupta, J. Johnson, L. Fei-Fei, S. Savarese, and A. Alahi, “Social gan: Socially acceptable trajectories with generative adversarial networks,” in *CVPR*, 2018, pp. 2255–2264.

[15] A. Sadeghian, V. Kosaraju, A. Sadeghian, N. Hirose, H. Rezatofighi, and S. Savarese, “Sophie: An attentive gan for predicting paths compliant to social and physical constraints,” in *Proceedings of the IEEE/CVF Conference on Computer Vision and Pattern Recognition*, 2019, pp. 1349–1358.

[16] V. Kosaraju, A. Sadeghian, R. Martín-Martín, I. Reid, S. H. Rezatofighi, and S. Savarese, “Social-bigat: Multimodal trajectory forecasting using bicycle-gan and graph attention networks,” *arXiv preprint arXiv:1907.03395*, 2019.

[17] J. Liang, L. Jiang, J. C. Niebles, A. G. Hauptmann, and L. Fei-Fei, “Peeking into the future: Predicting future person activities and locations in videos,” in *CVPR*, 2019, pp. 5725–5734.

[18] J. Liang, L. Jiang, K. Murphy, T. Yu, and A. Hauptmann, “The garden of forking paths: Towards multi-future trajectory prediction,” in *CVPR*, 2020, pp. 10 508–10 518.

[19] K. Mangalam, H. Girase, S. Agarwal, K.-H. Lee, E. Adeli, J. Malik, and A. Gaidon, “It is not the journey but the destination: Endpoint conditioned trajectory prediction,” in *European Conference on Computer Vision*. Springer, 2020, pp. 759–776.

[20] N. Shafee, T. Padir, and E. Elhamifar, “Introvert: Human trajectory prediction via conditional 3d attention,” in *Proceedings of the IEEE/CVF Conference on Computer Vision and Pattern Recognition*, 2021, pp. 16 815–16 825.

[21] C. Yu, X. Ma, J. Ren, H. Zhao, and S. Yi, “Spatio-temporal graph transformer networks for pedestrian trajectory prediction,” in *European Conference on Computer Vision*. Springer, 2020, pp. 507–523.

[22] Y. Yuan, X. Weng, Y. Ou, and K. Kitani, “Agentformer: Agent-aware transformers for socio-temporal multi-agent forecasting,” *arXiv preprint arXiv:2103.14023*, 2021.

[23] D. Helbing and P. Molnar, “Social force model for pedestrian dynamics,” *Physical review E*, vol. 51, no. 5, p. 4282, 1995.

[24] A. Vaswani, N. Shazeer, N. Parmar, J. Uszkoreit, L. Jones, A. N. Gomez, Ł. Kaiser, and I. Polosukhin, “Attention is all you need,” in *Advances in neural information processing systems*, 2017, pp. 5998–6008.

[25] J. F. P. Kooij, N. Schneider, F. Flohr, and D. M. Gavrila, “Context-based pedestrian path prediction,” in *European Conference on Computer Vision*. Springer, 2014, pp. 618–633.

[26] A. Bhattacharyya, M. Fritz, and B. Schiele, “Long-term on-board prediction of people in traffic scenes under uncertainty,” in *Proceedings of the IEEE Conference on Computer Vision and Pattern Recognition*, 2018, pp. 4194–4202.

[27] O. Styles, A. Ross, and V. Sanchez, “Forecasting pedestrian trajectory with machine-annotated training data,” in *2019 IEEE Intelligent Vehicles Symposium (IV)*. IEEE, 2019, pp. 716–721.

[28] R. Chandra, U. Bhattacharya, A. Bera, and D. Manocha, “Traphic: Trajectory prediction in dense and heterogeneous traffic using weighted interactions,” in *Proceedings of the IEEE/CVF Conference on Computer Vision and Pattern Recognition*, 2019, pp. 8483–8492.

[29] O. Makansi, O. Cicek, K. Buchicchio, and T. Brox, “Multimodal future localization and emergence prediction for objects in egocentric view with a reachability prior,” in *Proceedings of the IEEE/CVF Conference on Computer Vision and Pattern Recognition*, 2020, pp. 4354–4363.

[30] K. Mangalam, E. Adeli, K.-H. Lee, A. Gaidon, and J. C. Niebles, “Disentangling human dynamics for pedestrian locomotion forecasting with noisy supervision,” in *Proceedings of the IEEE/CVF Winter Conference on Applications of Computer Vision*, 2020, pp. 2784–2793.

[31] P. Gujjar and R. Vaughan, “Classifying pedestrian actions in advance using predicted video of urban driving scenes,” in *2019 International Conference on Robotics and Automation (ICRA)*. IEEE, 2019, pp. 2097–2103.

[32] B. Liu, E. Adeli, Z. Cao, K.-H. Lee, A. Shenoi, A. Gaidon, and J. C. Niebles, “Spatiotemporal relationship reasoning for pedestrian intent prediction,” *IEEE Robotics and Automation Letters*, vol. 5, no. 2, pp. 3485–3492, 2020.

[33] Y. Yao, M. Xu, Y. Wang, D. J. Crandall, and E. M. Atkins, “Unsupervised traffic accident detection in first-person videos,” in *2019 IEEE/RSJ International Conference on Intelligent Robots and Systems (IROS)*. IEEE, 2019, pp. 273–280.

[34] T. Yagi, K. Mangalam, R. Yonetani, and Y. Sato, “Future person localization in first-person videos,” in *CVPR*, June 2018.

[35] O. Styles, V. Sanchez, and T. Guha, “Multiple object forecasting: Predicting future object locations in diverse environments,” in *Proceedings of the IEEE/CVF Winter Conference on Applications of Computer Vision*, 2020, pp. 690–699.

[36] J. Qiu, F. P.-W. Lo, X. Gu, Y. Sun, S. Jiang, and B. Lo, “Indoor future person localization from an egocentric wearable camera,” *IROS*, 2021.

[37] R. Xiong, Y. Yang, D. He, K. Zheng, S. Zheng, C. Xing, H. Zhang, Y. Lan, L. Wang, and T. Liu, “On layer normalization in the transformer architecture,” in *International Conference on Machine Learning*. PMLR, 2020, pp. 10 524–10 533.

[38] C. Campos, R. Elvira, J. J. G. Rodríguez, J. M. Montiel, and J. D. Tardós, “Orb-slam3: An accurate open-source library for visual, visual-inertial, and multimap slam,” *IEEE Transactions on Robotics*, 2021.

[39] Y. Xiu, J. Li, H. Wang, Y. Fang, and C. Lu, “Pose Flow: Efficient online pose tracking,” in *BMVC*, 2018.

[40] H. Zhao, J. Shi, X. Qi, X. Wang, and J. Jia, “Pyramid scene parsing network,” in *CVPR*, 2017, pp. 2881–2890.

[41] C. Godard, O. Mac Aodha, M. Firman, and G. J. Brostow, “Diving into self-supervised monocular depth prediction,” October 2019.

[42] L. Van der Maaten and G. Hinton, “Visualizing data using t-sne.” *Journal of machine learning research*, vol. 9, no. 11, 2008.

[43] B. Zhou, H. Zhao, X. Puig, T. Xiao, S. Fidler, A. Barriuso, and A. Torralba, “Semantic understanding of scenes through the ade20k dataset,” *International Journal on Computer Vision*, 2018.

[44] D. P. Kingma and J. Ba, “Adam: A method for stochastic optimization,” *arXiv preprint arXiv:1412.6980*, 2014.